Impact of Different Noise Sources on the Performance of PIN- and APD-based FSO Receivers

Fang Xu[1], Mohammad-Ali Khalighi[2], Salah Bourennane[2]
[1]Commercial Aircraft Corporation of China Ltd. (COMAC), Shanghai, China
[2]École Centrale Marseille, Institut Fresnel, UMR CNRS 6133, Marseille, France
Xufang@comac.cc, {Ali.Khalighi, Salah.Bourennane}@fresnel.fr

***Abstract*— P-i-N (PIN) diodes and avalanche photo-diodes (APD) are the most commonly used photo-detectors in terrestrial FSO systems. In this paper, we review the photo-detection process for the cases of PIN- and APD-based receivers and provide a comprehensive study of different noise sources that affect signal detection in an FSO system. We present a complete and precise model for the receiver noise by taking different receiver parts into account. In particular, we study the impact of thermal, shot, background, and transmitter noises on the receiver performance by considering practical and realistic case studies. We bring clearance on the impact of the interaction of signal and background noise due to non-linear characteristic of the photo-detector, and on the role of the trans-impedance load resistance. We discuss the dominant noise components for the cases of using a PIN or an APD, and compare their performances at the presence or not of background radiations.**

I. Introduction

Free Space Optics (FSO) is a promising solution for very high data rate point-to-point communication [1], [2], [3], [4]. By FSO, the information-bearing laser beam is projected onto the optical receiver along the line of sight. At the receiver, the transmitted optical signal is converted to an electrical one thanks to a photo-detector (PD). Concerning the PD, solid-state devices are mostly used in commercial FSO systems since the quantum efficiency of phototube devices is too low for the commonly-used wavelengths [5]. The solid-state PD can be a P-i-N (PIN) diode or an avalanche photo-diode (APD). PIN diodes are usually used for FSO systems working at ranges up to a few kilometers [6]. The main drawback by using PIN PDs is that the receiver becomes thermal noise-limited. For long distance links, APDs are mostly used which provide a current gain thanks to the process of impact ionization. The drawback of APDs, in turn, is the excess noise at their output, which models the random phenomenon behind the generation of secondary photo-electrons.

In this work, we firstly review the photo-detection process and the different noise sources that affect signal detection in the case of terrestrial FSO systems. We consider two cases where a PIN or an APD is employed at the receiver and explain the statistical modeling of different noises.

Several previous works have considered, directly or indirectly, the receiver noise effect in optical communication systems. We cite here some works that have considered the noise modeling. These works, however, either use more or less simplified models for the receiver noise or consider a very different context from terrestrial FSO systems: Sorensen *et al.* numerically evaluated in [7] the performance of an APD-based optical receiver by considering only shot-noise and thermal noise. Leeb analyzed in [8] the effect of background radiations on the signal-to-noise ratio for direct and heterodyne/homodyne receivers in optical space links. In a previous work, we studied the impact of background radiations on the performance of FSO systems and proposed to use two laser wavelengths and differential data detection to reduce its effect [9], [10]. Also, we studied in [11] the spatial diversity receivers for thermal- and background-noise-limited receivers. Dolinar *et al.* studied in [12] the capacity of PPM channel in the case of using an APD and in the absence of scintillation. In [13], Srinivasan and Vilnrotter considered the use of APD-based detector arrays for space-to-ground optical communication systems. Manor and Arnon investigated in [14] the wavelength dependence of the performance of FSO systems using a PIN diode under different weather conditions. Kiasaleh studied the optimal average APD gain for the case of pulse position modulation (PPM) in [15]. Also, Cole and Kiasaleh considered the use of APD detector arrays for the cases of binary PPM and on-off keying (OOK) modulations in [16]. Lastly, Cvijetic *et al.* considered in [17] the impact of spatial diversity in a channel subject to turbulence for the two cases of PIN and APD detectors.

In contrast to these previous works, here we provide a complete and precise noise model for terrestrial FSO systems by taking into account the functions of the PD, the trans-impedance (TZ) circuitry, and the receiver low-pass filter (LPF). We study the impact of different noise sources on the receiver performance. In particular, we focus on the impact of background noise (also called background radiation or ambient noise) and on the role of the TZ load resistance, and discuss the dominant noise factor in different practical conditions, as well as the adequate choice of the PD type.

It is well known that the performance of FSO links is subject to other inhibitors such as propagation loss due to beam divergence, meteorological phenomena, and atmospheric turbulence or scintillation, to mention only a few. To focus on the noise effect, however, we consider

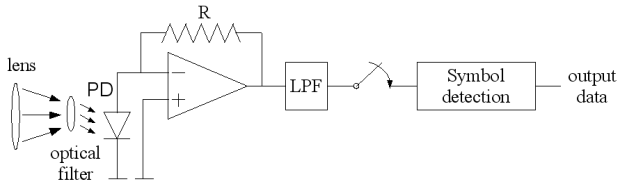

Fig. 1. The general block diagram of the receiver.

clear atmospheric conditions and perfect alignment between the transmitter and the receiver. Also, we consider a *normalized channel*, that is, we neglect the propagation loss.

The remainder of this paper is organized as follows. In Section II, we specify our assumptions and the main parts of the receiver. Also, we describe the optical field reception and present a statistical model for the number of received photons on the PD. Next, different noise sources affecting the receiver performance in the cases of PIN- and APD-based photo-detection are detailed in Sections III and IV, respectively. Signal detection is explained in Section V. Some numerical results are provided in Section VI, and Section VII concludes the paper.

II. Assumptions and General Receiver Model

We do not consider any kind of spatial, temporal or wavelength diversity. Intensity modulation and direct detection (IM/DD) is used based on the non-return to zero (NRZ) OOK modulation. In this way, the emission of an optical pulse of power P_t and duration T_s represents a bit 1 (ON state), whereas the absence of light for the same duration represents a bit 0 (OFF state). We do not consider any channel coding in this work.

A. Receiver main blocks

The general block diagram of the receiver is shown in Fig. 1. The receiver front end consists of a lens and optical filters. The lens has the role of collecting and focusing the received beam onto the PD surface. Note that in addition to the useful signal, the receiver lens also collects some undesirable background radiations. Background radiation may consist of direct sunlight (up to 10 mW, typically during sunrise or dawn), reflected sunlight (about hundreds of μW), or scattered sunlight from hydrometeor or other objects (about several μW) [5], [18], [19], [20]. The optical filers, employed prior to PD, perform spatial and spectral optical filtering to reduce the background noise level. The optical filter has a bandwidth B_0 of several nanometers typically.

Then, the PD, which can be a PIN or an APD, converts the received intensity to an electrical current i. The PD output current is next converted to a voltage by means of a TZ circuit, usually a low-noise Op-Amp with a load resistor R. The resistance of R is determined based on criteria such as the transmission rate, the dynamic range of the converted electrical signal, and the generated receiver thermal noise. It can be chosen about several hundreds of KΩ in deep-space applications [12] down to about 50-100 ohms in very high rate FSO links [17].

The receiver electronic circuitry adds some thermal noise onto the signal. The output of the TZ circuit is then passed through a low-pass filter (LPF) in order to limit the thermal and background noise level. The bandwidth B of the LPF is determined by the transmission rate $R_b = 1/T_s$; we take $B \approx R_b/2$. After clock recovery, sampling, and analog-to-digital conversion, we perform signal detection based on the maximum *a posteriori* (MAP) criterion. Details on signal detection will be provided later in Section V after reviewing the photo-detection process and specifying the statistical models of different noise sources for the cases of PIN and APD in Sections III and IV. Before that, we recall the general statistical model for the number of received photons at the PD, which is independent of the PD type.

Note that we assume perfect time synchronization of the system. Also, we assume that there is no spreading of the signal intensity across the symbols and we do not have any inter-symbol interference (ISI).

B. Number of received photons on the PD

We consider the single-mode plane-wave model for the incident optical signal. Assume that we receive an optical field $f_r(t,r)$ at the receiver's aperture area A. In fact, as mentioned previously, in addition to the useful signal, the receiver lens also collects some undesirable background radiations. We may perform spatial and spectral optical filtering at the receiver to limit the background noise level. However, even with good spatial and narrow-band filtering, a non-negligible background noise falls within the spatial and frequency ranges of the detector and limits the performance of the system by causing a variable offset in the converted electrical signal [10], [19]. Let us denote the desired signal and the background noise fields by $f_s(t,r)$ and $f_b(t,r)$, respectively. Then, we have,

$$f_r(t,r) = f_s(t,r) + f_b(t,r) \quad , \quad r \in A. \qquad (1)$$

Note that the PD can be considered as a square-law envelope detector. Let us denote the field complex envelopes corresponding to the useful signal field $f_s(t,r)$ and the background noise field $f_b(t,r)$ by $s(t)$ and $b(t)$, respectively. For the sake of notational simplicity, we do not specify the time index t. Considering normalized receiver's aperture area for simplicity (i.e., taking $A = 1$), the photo-detector *count rate* process ζ is [5]:

$$\zeta = \frac{1}{h\nu} \, |s+b\,|^2 = \frac{1}{h\nu}\Big[\,|s|^2 + |b|^2 + 2\;\Re\{sb^*\}\Big] \;, \quad (2)$$

where h is Planck's constant, ν is the optical frequency and $\Re\{.\}$ is the real part operator. Then, during the symbol time interval T_s, the mean number of photons $\bar{n}$ received at the photo-detector is:

$$\bar{n} = \int_0^{T_s} \zeta dt = \frac{1}{h\nu} \int_0^{T_s} \Big[\,|s|^2 + |b|^2 + 2\;\Re\{sb^*\}\Big] dt \;\cdot \qquad (3)$$

Note that the time average of the last term in (3) is equal to zero. We denote the received optical power corresponding to the useful signal by P_s, the background noise unilateral power spectral density by N_b, and the

collected optical power by $P_b = N_b\, B_0$. Since $P_s = |s|^2$ and $P_b = |b|^2$, (3) turns to:

$$\bar{n} = \frac{T_s(P_s + P_b)}{h\nu}. \tag{4}$$

So, the mean number of photons is directly proportional to the sum of the signal power and the background noise power.

Even if the received optical intensity is constant, the number n of absorbed photons by the PD is random and usually modeled by an ergodic and wide-sense stationary Poisson random process with the following probability mass function (PMF):

$$p(n) = \frac{\bar{n}^n e^{-\bar{n}}}{n!}. \tag{5}$$

If the mean number of absorbed photons $\bar{n}$ is relatively large, the Poisson process can be approximated with a Gaussian process [21]. In most FSO systems, the received photon flux is important enough to allow this approximation. So, setting $\sigma_n = \sqrt{\bar{n}}$, we have:

$$p(n) \approx \frac{1}{\sqrt{2\pi}\sigma_n} \exp\left(-\frac{(n-\bar{n})^2}{2\,\sigma_n^2}\right). \tag{6}$$

III. Noise sources for PIN-based receivers

Details on the noise in PDs can be found in [5], [21], [22], for instance. Different noise sources that we should deal with are: photo-current shot-noise which arises from input signal and/or background radiations, dark current, thermal noise, and the transmitter noise.

A. Photo-current shot noise

For a PIN diode, when an incident photon of sufficient energy strikes the diode, it generates a free electron-hole pair with a probability η. This probability, also known as the quantum efficiency, depends on both the photosensitive material and the optical wavelength. The generated free electrons flow across the junction gap and a photo-current is produced. Denoting the average number of generated electron-hole pairs that contribute to the detector current by $\bar{m}$, we have $\eta = \frac{\bar{m}}{\bar{n}}$. The random fluctuation of the current flowing through the device is usually called photo-current shot noise and considered as arising from the quantum noise effect. To calculate the variance of this shot noise, we should take the non-linear function of the PD and the LPF into account and present the formulation of the shot-noise current following the approach in [5].

We first calculate the auto-correlation function of ζ, $R_\zeta(\tau) = \mathrm{E}\{\zeta(t)\zeta(t-\tau)\}$, where $\mathrm{E}\{.\}$ denotes the expected value. Assuming that the background noise field is a stationary zero-mean complex Gaussian process, uncorrelated with the signal field, we obtain:

$$R_\zeta(\tau) = \left(\frac{1}{h\nu}\right)^2 \Big[2P_sP_b + R_{|s|^2}(\tau) + R_{|b|^2}(\tau) + R_{sb}(\tau)\Big], \tag{7}$$

where $R_{|s|^2}(\tau)$, $R_{|b|^2}(\tau)$ and $R_{sb}(\tau)$ are, respectively, the auto-correlation functions of the signal field intensity, that of the background field intensity, and the cross-correlation between these fields. Then, we take the Fourier transform of $R_\zeta(\tau)$ to obtain the power spectral density of ζ that we denote by $S_\zeta(f)$.

$$S_\zeta(f) \approx \left(\frac{1}{h\nu}\right)^2 (P_s+P_b)^2\,\delta(f) + \left(\frac{1}{h\nu}\right)^2 \Big[2P_sN_b + N_b^2\Big] \tag{8}$$

The two terms in brackets in (8) are the contribution from the interaction of signal with background radiation, and background radiation with itself. We consider now the PD output current i by taking into account the quantum efficiency η and the LPF inserted after the transimpedance circuit. Lets denote the transfer function of the LPF by $H(f)$ and its bandwidth by B. It can be shown that the power spectral density $S_i(f)$ of the PD output current is given by [5]:

$$S_i(f) = e^2\ |H(f)|^2\ \big[\,\eta\,\bar{\zeta} + \eta^2 S_\zeta(f)\,\big], \tag{9}$$

where e is the electron charge. As B is too small compared to the optical filter bandwidth B_0, we can in fact assume that the convolved spectra are almost flat within B. Also, we assume an ideal LPF with $|H(f)| \approx 1$ for $|f| \le B$. So, we obtain:

$$\begin{aligned} S_i(f) \approx\ & e^2\Big[\ \left(\frac{\eta}{h\nu}\right)^2 (P_s+P_b)^2\delta(f) + \frac{\eta}{h\nu}(P_s+P_b) \\ & +\ \left(\frac{\eta}{h\nu}\right)^2 (N_b^2 + 2P_sN_b)\ \Big] \end{aligned} \tag{10}$$

The term appearing with $\delta(f)$ corresponds to the square of the average generated photo-current I:

$$I = \frac{\eta(P_s+P_b)e}{h\nu} = I_s + I_b, \tag{11}$$

where we have defined I_s and I_b, the average photo-currents generated by the useful signal and by the background radiations, respectively. The other terms in (10) refer to the random component of i that we call the photo-current shot noise and denote its variance by σ^2_{sh}:

$$\begin{aligned} \sigma^2_{\text{sh}} &= 2e^2B\Big[\frac{\eta}{h\nu}(P_s+P_b) + \left(\frac{\eta}{h\nu}\right)^2 (N_b^2 + 2P_sN_b)\Big] \\ &= 2\,e\,(I_s+I_b)B + \frac{2\,I_b^2B}{B_0} + \frac{4\,I_s\,I_b\,B}{B_0} \end{aligned} \tag{12}$$

Note that most related works consider only the first term and set σ^2_{sh} to $2\,e\,(I_s+I_b)B$ without justifying it. We will later show that the two last terms in (12) can effectively be neglected in most practical cases.

B. Dark current

Besides the photo-current shot noise, we have another source of shot noise that consists of random fluctuations of the leakage current generated by the bias voltage applied to the PIN diode and is called *dark* current. This dark current is the sum of the diode surface leakage current and the bulk leakage current. Denoting the average dark current by I_{D}, the average surface leakage current by I_{DS} and the average bulk leakage current by I_{DB}, we have $I_{\text{D}} = I_{\text{DS}} + I_{\text{DB}}$. The variance of the dark current is [23]:

$$\sigma^2_{\text{dark}} = 2\,e\,(I_{\text{DS}} + I_{\text{DB}})B. \tag{13}$$

Note that sometimes shot-noise and dark current are called external and internal quantum noises, respectively [24]. Typical values for I_D vary from 1 to 10 nA for Si-based PIN, from 50 to 500 nA for Ge-based PIN, and from 1 to 20 nA for InGaAs-based PIN [23].

C. Thermal noise

A thermal noise component is also associated to a PIN PD by considering a certain shunt resistance R_s which is typically on the order of 100 KΩ to 1 GΩ. The corresponding *internal* noise is then considered as a zero-mean Gaussian process of variance σ^2_{shunt}:

$$\sigma^2_{\text{shunt}} = \frac{4KTB}{R_s}, \tag{14}$$

where T is the temperature in Kelvin and K is the Boltzmann constant. In addition to the PD, the receiver electronic circuitry also adds some noise onto the signal which consists principally of thermal and shot noise. The latter component is negligible compared to the former, however. The thermal noise is mainly caused by the load resistor R and is modeled as a zero-mean Gaussian process of variance σ^2_{load}:

$$\sigma^2_{\text{load}} = \frac{4KTB}{R}. \tag{15}$$

The post-amplification and LPF circuitry also add some thermal noise to the signal. To take it into account, usually an equivalent noise temperature T_e is considered in the above expression of σ^2_{load} instead of T.

D. Transmitter noise

Lastly, we should take the transmitter noise into account. In fact, in practice, the power level of the laser is unstable and the corresponding intensity fluctuations at the receiver are taken into account by considering the so-called laser relative intensity noise (RIN). The induced fluctuations on the photo-current i are usually considered as a kind of shot noise with the variance $\sigma^2_{\text{RIN}} = \text{RIN}\, I_s^2 B$. Typical values for RIN are between -110 dB/Hz and -140 dB/Hz for VCSEL lasers, between -120 dB/Hz and -140 dB/Hz for FP lasers, and between -150 dB/Hz and -165 dB/Hz for DFB lasers [25], [26].

E. Putting them all together

At the PD output, we have the contribution of all noise sources presented above. The distribution of the output current i can be approximated by a Gaussian that we denote by $\mathcal{N}(\mu_0, \sigma_0^2)$ and $\mathcal{N}(\mu_1, \sigma_1^2)$ for the cases of OFF- and ON-OOK symbols, respectively. We have:

$$\begin{cases} \mu_0 &= I_b + I_{\text{DS}} + I_{\text{DB}}, \\ \sigma_0^2 &= \sigma^2_{\text{sh}} + \sigma^2_{\text{dark}} + \sigma^2_{\text{shunt}} + \sigma^2_{\text{load}} \\ &= 2\,e\,(I_b + I_{\text{DS}} + I_{\text{DB}})B + \frac{2I_b^2 B}{B_0} + \frac{4KTB}{R_s} + \frac{4KT_eB}{R} \end{cases} \tag{16}$$

$$\begin{cases} \mu_1 &= I_s + I_b + I_{\text{DS}} + I_{\text{DB}}, \\ \sigma_1^2 &= \sigma^2_{\text{sh}} + \sigma^2_{\text{dark}} + \sigma^2_{\text{shunt}} + \sigma^2_{\text{load}} + \sigma^2_{\text{RIN}} \\ &= 2e(I_s + I_b + I_{\text{DS}} + I_{\text{DB}})B + \frac{2\,I_b^2 B}{B_0} + \frac{4\,I_s I_b B}{B_0} \\ &\quad + \frac{4KTB}{R_s} + \frac{4KT_eB}{R} + \text{RIN}\, I_s^2 B \end{cases} \tag{17}$$

IV. Noise model for APD-based receivers

An APD involves an avalanche multiplication in the photo-detection process [21]. More than one electron-hole pair are hence generated for each absorbed photon and the resulting accumulated current flow can be many times larger than that for a PIN. This amplification process that provides an internal gain is random in nature. The average APD gain that we denote here by G depends on the bias voltage and is typically in the range of 10 to 200 [5]. Like for PIN diodes, we have again the four noise sources of photo-current shot-noise, dark current, thermal noise, and the transmitter noise. Modeling these sources is different from the previous case, however, and should take into account the special APD photo-detection process.

A. Photo-current shot noise

Consider that during T_s, the APD receives an optical intensity P_r, comprising a signal intensity of P_s and an ambient light intensity of P_b: $P_r = P_s + P_b$. As for the case of a PIN diode, the actual number of absorbed photons n (also known as the *primary* count) is a Poisson random variable of mean $\bar{n}$, with the distribution given by (5). In response to these n photons, the APD generates at its output m electrons with the conditional probability distribution $p(m|n)$, which is derived by McIntyre in [27] and experimentally verified by Conradi in [28]:

$$p(m|n) = \frac{n\,\Gamma(\frac{m}{1-\varsigma}+1)}{m\,(m-n)!\,\Gamma(\frac{\varsigma m}{1-\varsigma}+n+1)} \times \left[\frac{1+\varsigma(G-1)}{G}\right]^{n+\frac{\varsigma m}{1-\varsigma}} \left[\frac{(1-\varsigma)(G-1)}{G}\right]^{m-n} \;;\; m \geq 1, \tag{18}$$

where $\Gamma(.)$ is the Gamma function and ς is the ionization ratio. Typical values for ς are between 0.002 to 0.06 for Si detectors, 0.7 to 1 for Ge detectors, and 0.4 to 0.7 for InGaAs detectors, respectively [23], [29]. Averaging the conditional probability distribution $p(m|n)$ over the Poisson-distributed n, we obtain the PMF of m, given the average number $\bar{n}$ of absorbed photons:

$$p(m|\bar{n}) = \sum_{n=1}^{\infty} p(m|n)p(n|\bar{n}). \tag{19}$$

An approximation to (19) has been derived by Webb [30] that provides a much simpler expression for analytical calculations:

ConTEL 2011, ISBN: 978-3-85125-161-6

$$p(m|\bar{n}) = \frac{1}{\sqrt{2\pi\bar{n}\,G^2F}\left(1+\frac{m-G\bar{n}}{\bar{n}GF/(F-1)}\right)^{3/2}} \times \exp\left(-\frac{(m-G\bar{n})^2}{2\,\bar{n}\,G^2F\left(1+\frac{m-G\bar{n}}{\bar{n}GF/(F-1)}\right)}\right) \;;\; m \geq \frac{-G\bar{n}}{F-1}, \tag{20}$$

where $F = \varsigma G + (2 - 1/G)(1 - \varsigma)$ is called the excess noise factor. When the skewness parameter $\delta^2 = \frac{\bar{n}F}{(F-1)^2}$ is large, the Webb distribution of (20) can be approximated by a Gaussian [30]. Taking the quantum efficiency η into account, the average generated photo-current I is:

$$I = I_s + I_b = \frac{G\eta(P_s + P_b)e}{h\nu}. \tag{21}$$

Also, the variance of the photo-current shot noise is [5]:

$$\sigma^2_{\text{sh}} = 2\,e\,GF(I_s + I_b)B + \frac{2\,I_b^2B}{B_0} + \frac{4\,I_sI_bB}{B_0}, \tag{22}$$

where we have also taken into account the interaction of signal intensity and background noise (the last two terms in (22)) as we explained for the case of the PIN diode.

B. Dark current

The output of APD also contains a dark current shot noise that is modelled as a Gaussian process like in the case of PIN. Here, the bulk leakage current is multiplied by the APD gain. The average dark current is hence $I_{\text{D}} = I_{\text{DS}} + G\,I_{\text{DB}}$ and its variance is given by:

$$\sigma^2_{\text{dark}} = 2\,e(I_{\text{DS}} + G^2F\,I_{\text{DB}})B \tag{23}$$

The typical values for I_{D} vary from 0.1 to 1 nA for Si-based APD, 50 to 500 nA for Ge-based APD, and 1 to 5 nA for InGaAs-based APD [23].

C. Thermal and transmitter noises

Similar to the case of PIN, we have the contribution of thermal noise from the TZ load resistor R and the electronic circuitry that is modelled by a zero-mean Gaussian process of variance $\sigma^2_{\text{load}} = 4KT_eB/R$. Note that, in contrast to the case of PIN, no shunt resistor is considered for APD. On the other hand, at the APD output, we have also current fluctuations due to the transmitter noise for ON symbols. By taking the APD excess noise factor into account, the corresponding noise variance is [31]:

$$\sigma^2_{\text{RIN}} = F\,\text{RIN}\,I_s^2B \tag{24}$$

D. Putting them all together

Taking all noise components into account, we can use the approximate Gaussian model for the APD output current that we denote by $\mathcal{N}(\mu_0, \sigma_0^2)$ and $\mathcal{N}(\mu_1, \sigma_1^2)$ in the cases of OFF- and ON-OOK symbols, respectively. We have:

$$\begin{cases} \mu_0 &= I_b + I_{\text{DS}} + G\,I_{\text{DB}} \\ \sigma_0^2 &= \sigma^2_{\text{sh}} + \sigma^2_{\text{dark}} + \sigma^2_{\text{load}} \\ &= 2\,e(GFI_b + G^2FI_{\text{DB}} + I_{\text{DS}})B + \frac{2I_b^2B}{B_0} + \frac{4KT_eB}{R} \end{cases} \tag{25}$$

$$\begin{cases} \mu_1 &= I_s + I_b + I_{\text{DS}} + G\,I_{\text{DB}} \\ \sigma_1^2 &= \sigma^2_{\text{sh}} + \sigma^2_{\text{dark}} + \sigma^2_{\text{load}} + \sigma^2_{\text{RIN}} \\ &= 2\,e(GF(I_s + I_b) + G^2FI_{\text{DB}} + I_{\text{DS}})B + \frac{2\,I_b^2B}{B_0} \\ &\quad + \frac{4I_sI_bB}{B_0} + \frac{4KT_eB}{R} + F\,\text{RIN}\,I_s^2B \end{cases} \tag{26}$$

V. Signal detection

Let us denote by x the transmitted OOK signal, which takes the values of 0 or 1, and the LPF output voltage by y. As we explained in the previous section, the ensemble of noise components at the PD output can be modelled by a Gaussian random process, either in the case of PIN or APD. As a result, we have the following general form for the conditional PDF of y:

$$P(y|x) = \frac{1}{\sqrt{2\pi}\sigma}\exp\left(\frac{-(y-\mu)^2}{2\sigma^2}\right). \tag{27}$$

For $x = 0$, we have $\mu = \mu_0R$ and $\sigma^2 = \sigma_0^2R^2$ given by (16) or (25), whereas for $x = 1$, we have $\mu = \mu_1R$ and $\sigma^2 = \sigma_1^2R^2$ given by (17) or (26). Note that the factor R is due to current-voltage conversion by the TZ circuit. We consider signal detection based on the MAP criterion by which the detected signal $\hat{x}$ is calculated as follows.

$$\hat{x} = \arg\max_x P(y|x)P(x) \tag{28}$$

Considering equiprobable symbols, i.e., $P(x) = 1/2$, (28) reduces to: $\hat{x} = \arg\max_x P(y|x)$. To obtain $\hat{x}$, we calculate the likelihood ratio (LR) of x as follows:

$$\text{LR} = \frac{P(y|x=1)}{P(y|x=0)} = \frac{\sigma_0}{\sigma_1}\exp\left(\frac{(y-\mu_0R)^2}{2\,\sigma_0^2R^2} - \frac{(y-\mu_1R)^2}{2\,\sigma_1^2R^2}\right). \tag{29}$$

If LR < 1, we set $\hat{x} = 0$; otherwise, we set $\hat{x} = 1$.

VI. Numerical results

Here we present some numerical results by considering realistic system parameters to study the impact of different noise components for the cases of PIN and APD. The system performance is evaluated in terms of average BER as a function of the optical transmit power P_t.

A. Simulation parameters

We consider two cases of a channel without atmospheric turbulence and a weak-turbulence channel. For the channel without atmospheric turbulence, we have $P_s = P_t$. For the latter case, we consider the Rytov variance of 0.04 in the Gamma-Gamma model [32]. We have $P_s = hP_t$ where h is the channel fading coefficient. Also, we consider a VCSEL laser working at $\lambda = 850$ nm and a data rate of $R_b = 1$ Gbps. Then, we have $T_s = 1/R_b = 1$ ns and $B \approx R_b/2 = 500$ MHz. We consider

Si-based PDs due to their high sensitivity around the considered wavelength. Without loss of generality, let us assume that the quantum efficiency is $\eta = 1$ for both PIN and APD. We assume that $T_e \approx T \approx 300\,\mathrm{K}$. For our Si-based APD, we consider $\varsigma = 0.007$ and $G = 100$. Also, for the TZ resistor, we consider two cases of $R = 100\,\Omega$ and $R = 10\,\mathrm{K}\Omega$, respectively. The first value is typical for very high-rate systems as it results in a short diode response time and also facilitates impedance matching with the ensuing RF front-end. The latter R value is typical for lower-rate systems. A larger R has the advantage of reducing the thermal noise and improving the receiver sensitivity.

B. Negligible noise components for PIN and APD

Since R_s is typically much larger than the load resistance R for a PIN diode, the thermal noise caused by R_s is negligible compared to that caused by R. Also, as we consider Si-based PDs, typical values for the average dark current I_D are about tens of nA. Therefore, the resulting shot-noise can practically be neglected for both cases of PIN and APD, although in the latter case the bulk leakage current is amplified by the APD gain G. Moreover, the noise component from the transmit laser is negligible as well, given the typical values of RIN for VCSEL lasers (see Subsection III-D).

On the other hand, the shot-noise components arising from the interaction of signal with background radiation and background radiation with itself due to the non-linear function of the PD are also practically negligible: In (12) and (22), the last two terms corresponding to the above mentioned components are negligible compared to the main shot-noise term. In fact, assuming a typical optical filter bandwidth B_0 of 1 nm which is equivalent to 3×10^{17} Hz, we have $(I_s I_b + I_b^2)/B_0 \ll e(I_s + I_b)$.

So, overall, the remaining important noise components on which we are going to focus, are the thermal noise, the PD shot-noise (including the excess noise of APD), and the background noise.

C. Negligible background noise conditions

Let us first consider the case where background radiations are negligible, i.e., $P_b \approx 0$. We have presented the receiver BER performances for the cases of PIN- and APD-based receivers in Fig. 2. We explain these results in the following subsections. Notice that, in practice, the guaranteed link BER for FSO systems is usually on the order of 10^{-9} or even lower. However, due to long Monte Carlo simulations, we have limited the results to BERs of about 10^{-6}.

1) Dominant noise for PIN and APD: We begin by studying the dominant noise components for PIN- and APD-based receivers by considering the no-turbulence regime. PIN-based receivers are usually considered as thermal-noise-limited. Let us check this point by looking for the required transmit power that we denote by $\tilde{P}_t$, for which the variance of the thermal noise σ^2_{load} equals that of shot noise σ^2_{sh} in (17). This way, we find $\tilde{P}_t = -20.7\,\mathrm{dBm}$ for the case of $R = 10\,\mathrm{K}\Omega$ and $\tilde{P}_t = -1.1\,\mathrm{dBm}$ for the case of $R = 100\,\Omega$. Obviously, for lower BERs or higher transmit power, shot noise dominates thermal noise. From Fig. 2 we notice that for BER$= 10^{-6}$, we have $P_t = -33.6\,\mathrm{dBm}$ for $R = 10\,\mathrm{K}\Omega$ and $P_t = -23.9\,\mathrm{dBm}$ for $R = 100\,\Omega$. Comparing to the corresponding $\tilde{P}_t$ calculated above, for $R = 10\,\mathrm{K}\Omega$, we have $P_t < \tilde{P}_t$. So, for practical BER values, the dominant component is thermal noise and the contribution of the shot noise is negligible. For $R = 100\,\Omega$, we have $P_t \ll \tilde{P}_t$ and the domination of thermal noise is incontestable.

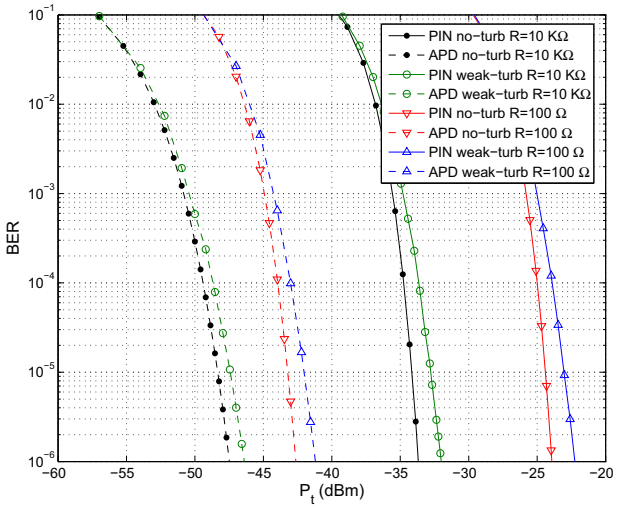

Fig. 2. Performance comparison for receivers using PIN and APD, $R = 100\,\Omega$ and $R = 10\,\mathrm{K}\Omega$, no-turbulence and weak-turbulence channels. Negligible background radiations.

On the other hand, APD-based receivers are usually considered as shot-noise-limited. To verify this point, we again look for the transmit power $\tilde{P}_t$ for which we have $\sigma^2_{\mathrm{load}} = \sigma^2_{\mathrm{sh}}$ from (26). We obtain $\tilde{P}_t = -65.4\,\mathrm{dBm}$ for $R = 10\,\mathrm{K}\Omega$ and $\tilde{P}_t = -45.4\,\mathrm{dBm}$ for $R = 100\,\Omega$. From Fig. 2, we notice that for $R = 10\,\mathrm{K}\Omega$, the BER is too high for P_t around $\tilde{P}_t$. Therefore, for practical P_t values (i.e., at practical BERs), the dominant component is the shot noise for this case. For $R = 100\,\Omega$, however, we have a BER of about 10^{-3} for $P_t = \tilde{P}_t$. So, although the dominant factor is the shot noise, the thermal noise still affects the receiver performance and is not really negligible.

2) Comparison of PIN and APD: We see from Fig. 2 that, as it could be expected, the overall performance of APD is better than that of PIN thanks to the APD gain. For example, considering the no-turbulence regime, if we set a desired BER of 10^{-6}, we have an improvement of about 18.7 and 13.8 dB in P_t by using an APD instead of a PIN for the cases of $R = 100\,\Omega$ and $R = 10\,\mathrm{K}\Omega$, respectively. Notice that, we would expect a gain of 20 dB in P_t due to the APD gain of $G = 100$. The reason for which we have a smaller gain here is the APD excess noise. Also, we notice that the improvement by using an APD instead of a PIN for $R = 10\,\mathrm{K}\Omega$ is less important than that for $R = 100\,\Omega$. In fact, the reduction of R results in an increase in the thermal noise level. The PIN

ConTEL 2011, ISBN: 978-3-85125-161-6

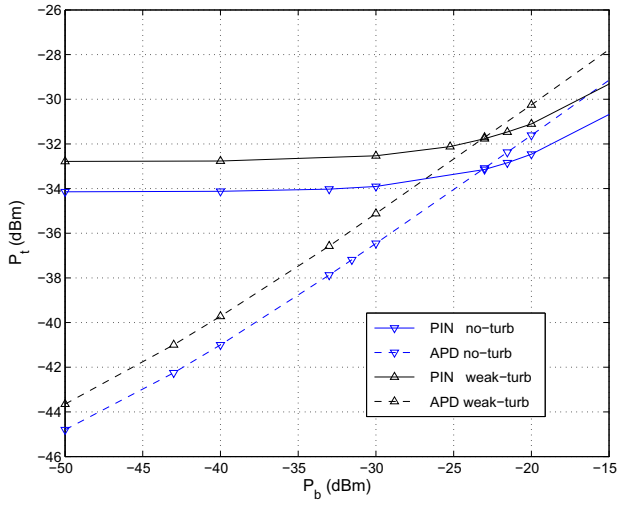

Fig. 3. Degradation of the receiver sensitivity due to background radiations, $R = 10\,\mathrm{K}\Omega$, no-turbulence and weak-turbulence channels, BER=10^{-5}.

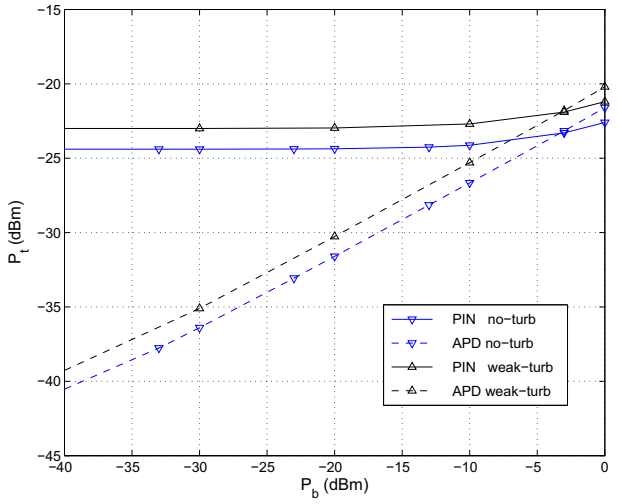

Fig. 4. Degradation of the receiver sensitivity due to background radiations, $R = 100\,\Omega$, no-turbulence and weak-turbulence channels, BER=10^{-5}.

is thermal noise-limited and it is more sensitive to the increased thermal noise than the shot noise-limited APD.

Similar conclusions can be drawn from Fig. 2 for the case of the weak-turbulence channel. The performance improvement by using an APD instead of a PIN is again significant: we have a gain of about 19 and 14.4 dB in P_t for $R = 100\,\Omega$ and $R = 10\,\mathrm{K}\Omega$, respectively.

D. Non-negligible background noise conditions

Here, we consider the case where the received optical intensity from background radiations P_b is not negligible. We are particularly interested to see the sensitivity of PIN- and APD-based receivers to background radiations. For this purpose, for each PD case, we evaluate the transmit power P_t that results in BER=10^{-5} for different background noise levels P_b. Figure 3 shows curves of P_t versus P_b for the cases of PIN and APD for $R = 10\,\mathrm{K}\Omega$ and for no-turbulence and weak-turbulence conditions. We notice that, compared to PIN, the performance of APD is more considerably affected by the background noise. That is because the background noise affects the receiver sensitivity as a kind of shot noise and, as we explained in Subsection VI-C, the performance of APD is limited by shot-noise. Interestingly, we notice that background noise can also become the dominant component in the case of using a PIN. This can be observed from Fig. 3: for both no-turbulence and weak turbulence conditions, by increasing P_b over -20 dBm, the P_t curves eventually have almost the same slope as those of APD. Another interesting point is that, for too large P_b (more than -23 dBm), the required P_t for APD exceeds that of PIN although it benefits from a gain of G. In other words, a PIN PD may be more suitable for a system working typically in relatively strong background radiations. The corresponding difference in P_t for the cases of PIN and APD is only about 2 dB, however. Notice that these conclusions do not depend on the turbulence regime.

Now consider Fig. 4 which contrasts the curves of P_t versus P_b for $R = 100\,\Omega$. We again note that for too large P_b, the required P_t for APD exceeds that of PIN. This occurs at about $P_b > -3$ dBm and the corresponding gain in P_t by using a PIN instead of an APD becomes negligible (less than 1 dB). Note that such conditions occur rarely in practice; typically it may happen when the receiver is exposed to direct sunlight.

VII. Conclusions

We reviewed in this paper different noise sources affecting signal detection when a PIN diode or an APD is employed at the receiver. We showed that the PD dark current, the noise components due to the instability of laser intensity, and the internal PIN thermal noise are practically negligible. We also showed that we can neglect the contributions from the interaction of the signal with background radiations due to non-linear characteristic of the PD. Compared to numerous works on FSO systems, here we provided a complete and precise model for the receiver noise for the case of terrestrial FSO systems and discussed the impact of different noise sources by considering realistic parameters related to practical application examples.

We confirmed that, when background noise is negligible, the PIN PD is thermal-noise-limited. Under such conditions, in order to reduce the thermal noise, we should choose the load resistor R as large as possible. In practice, we are limited by the response time of the photo-diode when working at very high data-rates. Impedance matching of the other receiver parts may also impose constraints on the choice of R. For the case of an APD, we should still choose a load resistance as large as possible, although in this case the receiver is shot-noise limited. In fact (as we explained in Section VI-C.1), for small R values, the thermal noise component still affects the receiver performance. It is true that the receiver performance is less affected by the choice of R

than for the case of using a PIN diode, however.

When background radiations are not negligible, an APD-based receiver is shot-noise limited obviously. For a PIN-based receiver, on the other hand, the limit of the background noise level P_b beyond which the receiver sensitivity is affected, depends on the load resistance. For larger R values, this limit is lower, that is, the receiver performance is more considerably affected by background radiations.

ACKNOWLEDGMENT

The authors wish to thank Profs. Hassan Akhouayri and Michel Lequime from Institut Fresnel, Marseille, and Frédéric Chazallet from Shaktiware Co., Marseille, France, for their fruitful discussions. This work was supported in part by the French PACA (Provence-Alpes-Côte d'Azur) Regional Council.

REFERENCES

[1] V. W. S. Chan, "Free-space optical communications," *Journal of Lightwave Technology*, vol. 24, no. 12, pp. 4750–4762, Dec. 2006.

[2] S. Bloom, E. Korevaar, J. Schuster, and H. Willebrand, "Understanding the performance of free-space optics," *Journal of Optical Networking*, vol. 2, no. 6, pp. 178–200, Jan. 2003.

[3] E. Leitgeb, M. S. Awan, P. Brandl, T. Plank, C. Capsoni, R. Nebuloni, T. Javornik, G. Kandus, S. S. Muhammad, F. Ghassemlooy, M. Loschnigg, and F. Nadeem, "Current optical technologies for wireless access," *ConTEL 2009-10th International Conference on Telecommunications*, pp. 7–17, June 2009, Zagreb, Croatia.

[4] S. Hranilovic, *Wireless Optical Communication Systems*, Springer, 2004.

[5] R. M. Gagliardi and S. Karp, *Optical Communications*, Wiley, second edition, 1995.

[6] *MRV website, Terescope product series*, http://www.mrv.com.

[7] N. Sorensen and R. Gagliardi, "Performance of optical receivers with avalanche photodetection," *IEEE Transactions on Communications*, vol. 27, no. 9, pp. 1315–1321, Sept. 1979.

[8] W. R. Leeb, "Degradation of signal to noise ratio in optical free space data links due to background illumination," *Applied Optics*, vol. 28, no. 16, pp. 3443–3449, Aug. 1989.

[9] M. A. Khalighi, Y. Jaafar, F. Xu, F. Chazallet, and S. Bourennane, "Double-laser differential signaling for suppressing background radiations in FSO systems," *Queen's 25th Biennial Symposium on Communications*, pp. 238–241, May 2010, Kingston, Canada.

[10] M. A. Khalighi, F. Xu, Y. Jaafar, and S. Bourennane, "Double-laser differential signaling for reducing the effect of background radiation in free-space optical systems," *IEEE/OSA Journal of Optical Communications and Networking*, vol. 3, no. 2, pp. 145–154, Feb. 2011.

[11] M. A. Khalighi, N. Schwartz, N. Aitamer, and S. Bourennane, "Fading reduction by aperture averaging and spatial diversity in optical wireless systems," *IEEE/OSA Journal of Optical Communications and Networking*, vol. 1, no. 6, pp. 580–593, Nov. 2009.

[12] S. Dolinar, D. Divsalar, J. Hamkins, and F. Pollara, "Capacity of pulse-position modulation PPM on gaussian and webb channels," *TMO Progress Report*, Aug. 2000.

[13] M. Srinivasan and V. Vilnrotter, "Avalanche photodiode arrays for optical communications receivers," *TMO Progress Report*, pp. 42–144, Feb. 2001.

[14] H. Manor and S. Arnon, "Performance of an optical wireless communication system as a function of wavelength," *Applied Optics*, vol. 42, no. 21, pp. 4285–4294, July 2003.

[15] K. Kiasaleh, "Performance of APD-based, PPM free-space optical communication systems in atmospheric turbulence," *IEEE Transactions on Communications*, vol. 53, no. 9, pp. 1455–1461, Sept. 2005.

[16] M. Cole and K. Kiasaleh, "Receiver architectures for the detection of spatially correlated optical field using avalanche photodiode detector arrays," *Optical Engineering*, vol. 47, no. 2, pp. 1–15, Feb. 2008.

[17] N. Cvijetic, S. G. Wilson, and M. Brandt-Pearce, "Performance bounds for free-space optical MIMO systems with APD receivers in atmospheric turbulence," *IEEE on Selected Areas in Communications*, vol. 26, no. 3, pp. 3–12, Apr. 2008.

[18] S. Bloom, E. Korevaar, J. Schuster, and H. Willebrand, "Understanding the performance of free-space optics," *Journal of Optical Networking*, vol. 2, no. 6, pp. 178–200, June 2003.

[19] D. Rollins, J. Baars, D. Bajorins, C. Cornish, K. Fischer, and T. Wiltsey, "Background light environment for free-space optical terrestrial communications links," *Proceedings of SPIE, Optical Wireless Communications*, vol. 4873, pp. 99–110, 2002.

[20] V. G. Sidorovich, "Solar background effects in wireless optical communications," *Proceedings of SPIE, Optical Wireless Communications*, vol. 4873, pp. 133–142, 2002.

[21] B. E. A. Saleh and M. C. Teich, *Fundamentals of Photonics*, Wiley, 1991.

[22] C. C. Davis, *Lasers and Electro-Optics: Fundamentals and Engineering*, Cambridge University Press, 1996.

[23] G. P. Agrawal, *Fiber-Optic Communications Systems*, Wiley, third edition, 1992.

[24] N. S. Kopeika and J. Bordogna, "Background noise in optical communication systems," *Proceedings of the IEEE*, vol. 58, no. 10, pp. 1571–1577, Oct. 1970.

[25] L. G. Zei, S. Ebers, J. R. Kropp, and K. Petermann, "Noise performance of multimode VCSELs," *Journal of Lightwave Technology*, vol. 19, no. 6, pp. 884–892, Jun. 2001.

[26] J. C. Whitaker, Ed., *The Electronics Handbook*, Taylor & Francis Group, second edition, 2005.

[27] R. McIntyre, "The distribution of gains in uniformly multiplying avalanche photodiodes: Theory," *IEEE Transactions on Electron Devices*, vol. 19, no. 6, pp. 703– 713, Jun. 1972.

[28] J. Conradi, "The distribution of gains in uniformly multiplying avalanche photodiodes: Experimental," *IEEE Transactions on Electron Devices*, vol. 19, no. 6, pp. 713– 718, Jun. 1972.

[29] "Avalanche photodiode a user guide," *PerkinElmer White Paper*, http://www.optoelectronics.perkinelmer.com.

[30] F. M. Davidson and X. Sun, "Gaussian approximation versus nearly exact performance analysis of optical communication systems with PPM signaling and APD receivers," *IEEE Transactions on Communications*, vol. 36, no. 11, pp. 1185–1192, Nov. 1988.

[31] A. L. Sanches, J. V. dos Reis, and B. H. V. Borges, "Analysis of high-speed optical wavelength/time CDMA networks using pulse-position modulation and forward error correction techniques," *Journal of Lightwave Technology*, vol. 27, no. 22, pp. 5134–5144, Nov. 2009.

[32] L. C. Andrews and R. L. Phillips, *Laser Beam Propagation Through Random Media*, SPIE Press, second edition, 2005.